

Title: *The evolution of borneol repellency in culicine mosquitoes*

Authors: Yuri Vainer^{1†}, Yinliang Wang^{1,5†}, Robert M. Huff^{2†}, Majid Ghaninia³, Iliano V. Coutinho-Abreu⁴, Evyatar Sar-Shalom¹, Carlos Ruiz⁷, Dor Perets¹, Esther Yakir¹, Dhivya Rajamanickam², Alon Warburg⁶, Philippos Papathanos¹, Omar S. Akbari⁴, Rickard Ignell³, Jeff A. Riffell⁷, R. Jason Pitts^{2§}, Jonathan D. Bohbot^{1§}

Authors affiliations:

1 Department of Entomology, The Hebrew University of Jerusalem, The Robert H. Smith Faculty of Agriculture, Food and Environment, Rehovot, Israel

2 Department of Biology, Baylor University, Waco, Texas, USA

3 Unit of Chemical Ecology, Department of Plant Protection Biology, Swedish University of Agricultural Sciences, Alnarp, Sweden

4 School of Biological Sciences, Department of Cell and Developmental Biology, University of California, San Diego, La Jolla, CA, USA

5 Northeast Normal University, China

6 Department of Microbiology and Molecular Genetics, Institute for Medical Research Israel-Canada, The Kuvim Centre for the Study of Infectious and Tropical Diseases, Faculty of Medicine, The Hebrew University of Jerusalem, Jerusalem, Israel

7 Department of Biology, University of Washington, Seattle, WA, USA 98195

† Yuri Vainer, Yinliang Wang and Robert M. Huff contributed equally to this work.

§ Co-corresponding authors

24 **Funding:** ISF 997/19 awarded to A.W., ISF 719/21 awarded to J.B., NIH RO1AI175152 and
 25 NSF IOS-2242604 awarded to O.S.A., NIH R01AI148300 awarded to J.A.R, O.S.A., and R.J.P.
 26 J.A.R was funded by the Bill and Melinda Gates Foundation (INV-021766). Science and
 27 Technology Development Plan Project of Jilin Province, China (20200402001NC) awarded to
 28 Y.W. This research was supported by the Ministry of Science & Technology, Israel to P.A.P.
 29 (grant numbers 3-16795 and 3-17985).

Abstract

Insects have developed remarkable adaptations to effectively interact with plant secondary metabolites and utilize them as cues to identify suitable hosts. Consequently, humans have used aromatic plants for centuries to repel mosquitoes. The repellent effects of plant volatile compounds are mediated through olfactory structures present in the antennae, and maxillary palps of mosquitoes. Mosquito maxillary palps contain capitate-peg sensilla, which house three olfactory sensory neurons, of which two are mainly tuned to either carbon dioxide or octenol - two animal host odorants. However, the third neuron, which expresses the OR49 receptor, has remained without a known ecologically-relevant odorant since its initial discovery. In this study, we used odorant mixtures and terpenoid-rich *Cannabis* essential oils to investigate the activation of OR49. Our results demonstrate that two monoterpenoids, borneol and camphor, selectively activate OR49, and OR9-expressing neurons, as well as the MD3 glomerulus in the antennal lobe. We confirm that borneol repels female mosquitoes, and knocking out the gene encoding the OR49 receptor suppresses the response of the corresponding olfactory sensory neuron. Importantly, this molecular mechanism of action is conserved across culicine mosquito species, underscoring its significance in their olfactory systems.

Key words: mosquitoes, borneol, monoterpenoid, repellent, odorant receptor, maxillary palp

1. Introduction

The use of plants to keep away insects has been a human practice since prehistorical times (Wadley et al., 2011) and is still a current practice in many parts of the world (Maia and Moore, 2011; Pålsson and Jaenson, 1999). This practice is shared with nonhuman primates that use

plants topically for their insect repelling properties (Baker, 1996). Plant-based essential oils (EOs), including lemon eucalyptus leaf oil (Moore and Debboun, 2007), citronella oil (Kongkaew et al., 2011), and coconut oil (Zhu et al., 2018) exhibit different degrees of repellent activity due to the presence of pyrethrins (Liu et al., 2021), phenol derivatives, and terpenoids (Iovinella et al., 2014). The latter chemical class includes oxygen-containing monoterpenes with open-chain hydrocarbons, such as linalool, citronellol, geraniol, and cyclic derivatives such as cineole, fenchone, camphor and borneol.

Borneol is believed to have derived its name from the island of Borneo, where it was initially traded with China and then introduced to the West due to its therapeutic, refreshing, and repellent effects against mosquitoes (Mei et al., 2023). Essential oils from various aromatic and medicinal plants such as *Salvia* spp. (Amer and Mehlhorn, 2006; Conti et al., 2012; Dayaram and Khan, 2016), *Valeriana officinalis* (Gordon et al., 2018), *Rosmarinus officinalis* (Alavez-Rosas et al., 2022; Dayaram and Khan, 2016; Drapeau et al., 2009; Pratiwi and Purwati, 2021), *Plectranthus* spp. (Kulkarni et al., 2013; Lukhoba et al., 2006), *Thymus* spp. (Pitarokili et al., 2011) and *Coriandrum sativus* (Benelli et al., 2013; Dayaram and Khan, 2016) contain significant levels of borneol that exhibit repellent and toxic activities against mosquito larvae (Santos et al., 2010).

Our understanding of the molecular modes of repellent action remains fragmented. Catnip oil, aside from its medical properties, exhibits repellency mediated by iridoids like nepetalactone, which target the transient receptor potential cation channel TRPA1 (Melo et al., 2021) and odorant receptors (Dickens and Bohbot, 2013) in insects. Similarly, the monoterpene citronella, the primary compound found in citronella oil, has been shown to target both the odorant receptor co-receptor (Orco) and the TRPA1 channel (Kwon et al., 2010).

Minimal information is available in the scientific literature regarding the molecular mode of action underlying borneol detection by insects. However, previous research has demonstrated that borneol, along with other monoterpenoids, induces Orco-mediated repellency in the antennae of *Ae. aegypti* (Andreazza et al., 2023; Liu et al., 2021). Interestingly, an additional mechanism for borneol-mediated repellency operates through a separate Orco-mediated pathway in the antennae of *Ae. aegypti* (Andreazza et al., 2023; Liu et al., 2021).

The capitae-peg (cp) sensillum located on the maxillary palp comprises three olfactory neurons, each distinguishable by size, olfactory receptor gene expression profile, and odor response characteristics. In both culicine and anopheline mosquitoes, the largest olfactory sensory neuron (cpA) expresses three gustatory receptors (*Grs*) that specifically detect CO₂ (Erdelyan and Mahood, 2011; McMeniman et al., 2014). The medium-sized cpB neuron of *Anopheles gambiae* and *Aedes aegypti* expresses the 1-octen-3-ol odorant receptor *Or8* and its co-receptor Orco (Grant and Dickens, 2011; Grant and O'Connell, 1996; Lu et al., 2007). Both CO₂ and 1-octen-3-ol elicit attraction and signal the presence of animal hosts in anopheline (Takken and Kline, 1989) and culicine (Gillies, 1980) mosquitoes. This functional organization has remained remarkably conserved throughout over 180 million years of mosquito evolution across these clades.

The third neuron (cpC) expresses a distinct *Or* gene in anopheline and culicine mosquitoes. In anophelines, the cpC neuron expresses the *Or28* gene (Lu et al., 2007), which responds to acetophenone and 2,4,5-trimethylthiazole, two plant volatile organic compounds (pVOC) (Wang et al., 2010). Conversely, in culicines, the cpC neuron expresses the *Or49* gene (Bohbot et al., 2007), which is unrelated to *AgamOr28*. Elucidating the function of OR49 within the capitae-

peg sensillum in mosquito palps will provide crucial insights into understanding the fundamental aspects of cp neuron compartmentalization (Su et al., 2012).

Using a pharmacological approach, we expressed *Or49* in a heterologous expression system and subjected it to odorant mixtures, plant EOs, and individual volatile odorant compounds. Our findings provide strong evidence that the OR49 receptor is responsive to plant-derived bicyclic monoterpenoids particularly showing a marked selectivity towards borneol—a well-known repellent compound that also exhibits toxicity to *Aedes* mosquito larvae. Furthermore, we observed that a loss-of-function mutation in the *Or49* gene leads to a lack of electrophysiological responses when stimulated by borneol in the cpC neuron. Confirming our pharmacological and electrophysiological results, behavioral studies reveal that borneol induces repellency in female mosquitoes seeking animal hosts. It is likely that mosquitoes employ borneol as a signal to distinguish between human and plant hosts. These findings highlight the pivotal role of OR49 in shedding light on the function of cp neuron compartmentalization.

Results

The conservation of the OR49 protein family spans across the evolutionary history of mosquitoes
Using the AegOR49 protein sequence as a query, we identified orthologs in *Ae. albopictus*, *Cx quinquefasciatus*, *Tx. amboinensis* and *An. gambiae* (Figure 1A). Protein sequence alignment shows high level of sequence coverage and a broad range of sequence identities that correlates with mosquito phylogenetic relationships (Figure 1B). Our phylogenetic analysis supports previous studies (Bohbot et al., 2007; Matthews et al., 2018) describing the OR49 family as a Culicinae-specific group (Figure 1C). The culicine OR49, OR29, OR71 groups and the more distantly related anopheline OR48/49 group form a monophyletic clade. These clades are further

supported by their exon structure and conserved intron phases (Figure 1D). The *Or49* genes are located on chromosome 2 in both *Aedes* and *Anopheles* mosquitoes (Figure 1E). In *Aedes* mosquitoes, *Or49* is located with *OR29* and *OR71* within several kb of each other and have conserved syntenic relationships with neighbouring genes (Figure 1F). Except for the close genomic proximity of OR49-related genes in *Cx. quinquefasciatus*, syntenic relationships in this region are not shared with *Aedes* genomes. By contrast, *Anopheles* homologs (*Or48/49*) are sitting next to each other, within a 5 kb distance of each other and without close neighboring *Or* genes.

OR49 is a selective borneol receptor

To identify candidate OR49 ligands, we used the two-electrode voltage clamp of oocytes expressing OR49 (Figure 2A, Table S1). We investigated the response of AalbOR49 to a panel of odorants, which included 81 organic compounds representing a range of chemical classes (Table S1). Oocytes expressing functional receptor complexes were strongly activated by blends containing ketonic compounds (see in inset in Figure 2B). Individual testing of the single compounds from the ketone blend revealed the efficacy of bicyclic monoterpenoids, with camphor emerging as the most efficacious member followed by cineole (also called eucalyptol) and fenchones (Figure 2B).

Subsequently, we screened OR49 from the nectar-feeding *Tx. amboinensis* (*TambOR49*) with 8 *Cannabis*-derived terpene mixtures (Figure 2C, Table S1, Figure S1). The three most active mixtures were Pineapple Haze, OG Kush, Adom #9 followed by Master Kush with a much lower efficacy. Six terpene sub-mixtures, each containing 3-4 terpenes present in all four active *Cannabis* essential oils, were further tested using a single-blind approach. Sub-mixture No. 2

was the only pharmacologically-active treatment (Figure 2D). Single compounds from mixture No. 2 were then prepared and individually tested in a single-blind approach as well. The racemic borneol was significantly more active than fenchol, alpha-terpineol, geraniol and camphor (Figure 2D). Subsequently, the borneol content in the original *Cannabis* mixtures was revealed, establishing a correlation between the borneol content and the activity of the blend (Figure 2C, Figure S2).

We established concentration-response curves (CRCs) to examine the relative sensitivity of mosquito OR49s for the two enantiomers of borneol. TambOR49 and AegOR49 did not exhibit enantioselectivity towards the (+) and (-)-borneol (Figure 2E) as indicated by their EC₅₀ values in the one-digit micromolar range. We established additional CRCs between TambOR49, *Cx. quinquefasciatus* OR38 (CquiOR49), *Ae. aegypti* OR49 (AegOR49), and *Ae. albopictus* OR49 (AalbOR49), for the two most potent ligands, (+)-borneol and (+)-camphor (Figure 2F). (+)-Borneol was 19-32 times more potent than (+)-camphor in all cases except for TambOR49 in which both compounds were equally active in the low micromolar range. In all four examined culicine species, including the nectar-feeding *Tx. amboinensis*, (+)-borneol consistently elicited significantly higher responses than (+)-camphor (Figure 2G).

In *An. gambiae*, the cpC neuron expresses OR28 (Figure 2A), which is activated by panel of diverse plant VOCs with acetophenone and 2,4,5-trimethylthiazole being the most effective ligands in the *Xenopus* oocyte expression system (Lu et al., 2007; Wang et al., 2010). The EC₅₀ values of AgamOR28 for acetophenone, α-pinene, α-terpineol and (+)-borneol were in the low millimolar range indicating that more potent ligands remain to be identified (Figure S4). Borneol did not elicit any response at the tested concentrations suggesting that AgamOR28 is tuned to VOCs belonging to different chemical classes.

The maxillary palp of culicine mosquitoes responds to borneol and camphor

To investigate the olfactory effect of camphor and borneol *in vivo*, we conducted electropalpogram (EPG) recordings on three culicine (*Ae. albopictus*, *Ae. aegypti*, *Cx. pipiens*) and one anopheline (*An. gambiae*) species. 1-Octen-3-ol, which served as a positive control, induced significant responses in all mosquitoes tested. Camphor and borneol elicited consistent palp responses in Culicinae mosquitoes, including *Ae. albopictus*, *Ae. aegypti*, and *Cx. pipiens* but not in *An. gambiae* (Figure 3). In *Ae. albopictus*, (–)-borneol was more active than (+)-camphor, while in *Ae. aegypti* both borneol enantiomers elicited significantly greater EPG responses than camphor enantiomers. In *Cx. pipiens*, borneol and camphor elicited comparable EPG responses.

We also established dose-response relationships with (+)-camphor and (+)-borneol in *Ae. albopictus*, *Ae. aegypti*, and *Cx. pipiens* (Figure 3B). Among the three culicine species, *Cx. pipiens* exhibited the largest responses in response to (+)-camphor. However, we did not find any significant statistical differences in activity between camphor and borneol in the tested species.

The Or49 gene confers sensitivity to borneol

To knock out the gene encoding the *Ae. aegypti* OR49 receptor, we used homology directed repair (HDR) to knock in a transgenic construct containing the QF2 transactivator and a ubiquitously expressing eCFP fluorescent marker driven by the OpiE2 promoter at the start codon of the *Or49* gene (Figure S5A,B). HDR was triggered by double strand breaks at the *Or49* promoter and the 1st exon mediated by two guide RNAs, whose cleavage activities had been tested *in vitro* (Figure S5C). Out of 739 injected embryos, 5.5% survived to the pupal stage.

These G_0 individuals were sex sorted and outcrossed with wildtypes. Sixteen G_1 larvae displayed blue (cyan) fluorescent bodies (Figure S5D). Insertion of the transgenes within *Or49* was confirmed in multiple G_1 individuals (Figure S5E,F) by sequencing of the insertion sites as well as the transgene (Figure S5E,F) resulting in a nonfunctional receptor. An *Or49*^{-/-} homozygous mosquito strain was isolated by single-pair mating, screening the fluorescence marker in the offspring for 100% penetrance, and PCR confirmation for the presence of homozygous mutant alleles (Figure S5G).

To investigate the genetic mechanism determining borneol sensitivity in the palp, we conducted single-sensillum recordings from the capitate-peg sensillum of *Ae. aegypti*, *Ae. albopictus*, *Cx. quinquefasciatus* and *An. gambiae* (Figure 4A, Figure S6). Single sensillum recordings identified the spontaneous activity of three sensory neurons, distinguished by differences in spike amplitudes, housed in the capitate peg sensilla of wild type *Ae. aegypti* (Figure 4C) and *An. gambiae* (Figure 4D). The response of the cpA and cpB neurons to CO₂ (Majeed et al., 2017) (data not shown) and *R*-(-)-1-octen-3-ol (Figure 4C; Majeed et al., 2016), respectively, has been well characterized in previous studies (Grant and Dickens, 2011; Grant and O'Connell, 1996; Lu et al., 2007). (+)-Borneol elicited a dose-dependent response in the cpC neuron of *Ae. aegypti*, *Ae. albopictus*, *Cx. quinquefasciatus* but not in *An. gambiae* s.s. (Figure 4B). No SSR responses were recorded from the cpC neuron in the *Ae. aegypti Or49* null mutant line in response to (+)-borneol (Figure 4C).

Two-photon imaging and borneol responses in the MD3 glomerulus

To examine how *Ae. aegypti* processes borneol in the antennal lobe (AL), two-photon imaging experiments were conducted using pan-neuronal GCaMP-expressing *Ae. aegypti* mosquitoes. We

utilized existing mosquito lines that contained a *QUAS-GCaMP6s* transgene crossed with the *brp-QF2* driver line (Zhao et al., 2022), allowing the directed expression of the calcium indicator GCaMP6s in all neurons of the AL. Mosquitoes were glued to holders that permitted two-photon imaging of calcium responses in the AL (Figure 5A), allowing repeatable registration of the AL glomeruli between preparations (Figure 5B) and recording of glomerular responses (Figure 5C) (Lahondere et al., 2020). Glomeruli from our two-photon imaging results were mapped to AL atlases (Shankar and McMeniman, 2021; Wolff et al., 2022), allowing accurate identification of the glomeruli of interest in their spatial context (Additional file 7). We focused on the mediodorsal glomeruli, as these glomeruli receive input from the capitate peg sensilla of maxillary palps (Figure 5B,C) and are responsive to host odors, including 1-octen-3-ol (MD2) and CO₂ (MD1) (Wolff et al., 2022).

To determine the odor coding of the mediodorsal glomeruli, and identify the cognate glomerulus representing borneol, we first recorded from the MD1-3 glomeruli while stimulating with CO₂ (5%), 1-octen-3-ol (10⁻⁴ dilution), borneol (10⁻⁴ dilution), and the solvent control. For the MD3 glomerulus, (+)-borneol elicited strong, tonic responses that were significantly greater than the solvent control (P<0.001) (Figure 5D). By contrast, responses of the MD1 and MD2 glomeruli to borneol were not significantly different from the control (P=0.09 and 0.23, respectively). The MD2 glomerulus showed the greatest responses to 1-octen-3-ol (Figure 5E) (P = 0.00003), and the MD1 glomerulus to CO₂ (P=0.01) (Figure 5F). Given MD3's response to (+)-borneol, and OR49 / cpC's responses to other terpene compounds, we next examined how this glomerulus responded to a limited panel of different odorants, including enantiomers of borneol and camphor. From this panel, (–)-borneol elicited the greatest response in the MD3 glomerulus (Figure 5G), closely followed by (+)-borneol and enantiomers of camphor.

Borneol repels human-host seeking female Ae. aegypti mosquitoes

To examine the impact of (+)-borneol on blood-seeking *Aedes aegypti* mosquitoes, we conducted an arm-in-a-cage assay, exposing 15 females to human skin odor for 10 minutes (Figure 6). A protective glove covered the hand, allowing mosquitoes to detect the odor through a dorsal open area. This open area was protected with a screen and equipped with a chemical holder for the deposition of (+)-borneol (1M). To monitor the number of females in the region of interest (ROI), we trained a custom object detection YOLOv5 model (Jocher et al., 2022). Our results showed a significant reduction (71.2%) in female landing on the ROI in the (±)-borneol-treated hand compared to the vehicle-treated hand when presented separately (Figure 6A). The (+)-borneol treatment consistently demonstrated lower detections, with less statistical variation between repetitions than the vehicle treatment (Figure S7A). In both the control and borneol treatments, we observed three waves of visits (Figure S7B). We used the trained YOLOv5 model to monitor mosquitoes present in the ROI over time (Figure 6B) for all repetitions see Figure S7C, and a video sample is available in Additional file 8. Figure S7B provides a visual representation of the variation in total detections per minute, highlighting the detection differences between the control and (+)-borneol treatments (total detections of 64,549 and 18,584, respectively) throughout the duration of the experiment. In the control treatment, the highest number of detections was observed in the one-two minutes interval, accounting for 16.2% of the total detections. In the (+)-borneol treatment, the peak detections occurred during at the 8-9 minute interval, comprising 14.4% of the total detections.

4. Discussion

Our results show that the culicine OR49 proteins are selective and sensitive bicyclic monoterpene receptors with a marked selectivity for borneol. Furthermore, we show that the deletion of the *Ae. aegypti Or49* gene suppresses cpC electrophysiological responses to borneol. In all three blood-feeding culicine species, OR49s were more sensitive to borneol than to camphor. Interestingly, the *Tx. amboinensis* OR49 exhibited overlapping sensitivity towards borneol and camphor suggesting that camphor plays an increased role in this species. However, camphor elicited significantly lower currents than borneol.

The OR49 clade is conserved in culicine mosquitoes. A complex process of gene duplication events appears to have generated several related ORs, including OR37, OR38, OR71 and others. Whether this OR subfamily expansion in culicines have specialized in detecting cyclic monoterpenes will have to be examined. Antennal-expressed *AgamOr48* (Hill et al., 2002), one of the two closest homologs to culicine *Or49*, responds to straight chain alcohols, ketones, and acetates (Carey et al., 2010; Wang et al., 2010) suggesting that anopheline are tuned to a different class of compounds of unknown ecological function.

In pharmacological assays, natural insect repellents interact with TRP channels (Melo et al., 2021) and ORs (Bohbot et al., 2011; Bohbot and Dickens, 2010; Dekel et al., 2019; Xu et al., 2019; Zeng et al., 2018) at the micromolar to low millimolar concentration range. By comparison, our results show that OR49s exhibit sensitivities three log units below these examples and is matched only by the *Drosophila melanogaster* OR56a-geosmin interaction (Stensmyr et al., 2012).

Contrary to the well-characterized mosquito OR8, which discriminates between the two 1-octen-3-ol enantiomers, the (+) and (–)-borneol elicited comparable activations at the pharmacological, physiological and AL levels. These findings suggest that the receptor binding

pocket accommodates both forms of borneol eliciting the activation of the MD3 glomerulus in the brain. These findings align with previous studies demonstrating that the three MD glomeruli receive input from the maxillary palp cp neurons whereby the MD1 glomerulus receiving CO₂ input from the cpA neurons (Anton et al., 2003) while the medium size MD2 glomerulus receives 1-octen-3-ol input from the cpB neurons (Wolff et al., 2023).

Borneol and camphor evoked lower responses than 1-octen-3-ol in the culicine palps, which is consistent with the smaller size of the cpC neuron in comparison to the cpB neuron. Based on single sensillum recordings, these responses of the palp can be directly attributed to the *Or49* gene. The absence of OR28 activation and *An. gambiae* palp EPG responses by borneol and camphor support this conclusion.

Borneol and borneol-rich plants have long been known not only for their medicinal use (Mei et al., 2023) but also for their insecticidal properties against the granary weevil (Kordali et al., 2006) and fire ants (Zhang et al., 2014). This monoterpenoid has also larvicidal properties against a variety of mosquito species (Afify and Galizia, 2014; Nunes et al., 2018; Pitarokili et al., 2011; Raj et al., 2015; Rajkumar and Jebanesan, 2010; Waliwitiya et al., 2009). Borneol repels fungus gnats (Cloyd et al., 2011), the booklouse *Liposcelis bostrychophila* (Liang et al., 2013) and fire ants (Zhang et al., 2014). It also influences adult mosquito behavior, repelling human host-seeking *Ae. aegypti*, *Cx. quinquefasciatus* and *An. stephensi* (Hwang et al., 1985; Pitarokili et al., 2011) while its presence in EOs stimulates oviposition in *Ae. aegypti* (Waliwitiya et al., 2009).

Is OR49 a molecular target of toxic plant-produced monoterpenoids, such as camphor and borneol, or do mosquito detect the volatile compounds in order to avoid their sources? Plants synthesize a variety of secondary metabolites to defend against herbivores and pathogens.

Bicyclic monoterpenoids, such as 1-8-cineole, fenchone, camphor and borneol, may act as acetylcholinesterase inhibitors (Abdelgaleil et al., 2009; Picollo et al., 2008). Other classes of terpenes have been proposed to target octopamine receptors (Enan, 2001) and the γ -aminobutyric acid (GABA) type A receptor (Höld et al., 2000). Their overall effects include developmental delays, oviposition and egg hatching reduction (Abdelgaleil et al., 2022). Intriguingly, gravid females exhibit a contrasting behavior, laying more eggs in solutions containing borneol and camphor (Waliwitiya et al., 2009), suggesting that these compounds have opposite effects on host-seeking behavior and the oviposition preferences of gravid female mosquitoes.

Mosquitoes seem to avoid plants emitting toxic levels of bicyclic monoterpenoids, with camphor and borneol ranking among the most potent compounds. This avoidance involves a dedicated olfactory circuit, beginning with OR49, a receptor expressed by the palp cpC neuron that projects to the MD3 glomerulus in the antennal lobe of *Ae. aegypti*. Whether borneol and other bicyclic monoterpenoids serve as danger or attractive signals, the cpC neuron may contribute to identify non-animal resources. Indeed, the significance of the stereotyped neuron combination in the cp sensillum in the maxillary palp of culicine is remarkable from an evolutionary and functional standpoint. The two largest neurons are tuned to animal host attractants whereas the smallest and third neuron responds to a plant host odorant with repellent activity. This antagonism in valence whereby attractive odorants is detected by the largest OSNs while repellent odorants are detected by small OSNs is widespread in animals (Ng et al., 2020). In this model, animal host odors are dominated by animal host odorants but can be modulated by the presence of an odor that signals alternative resources such as a plant host or a source of danger.

Innate repellency such as the one mediated by the OR49-borneol-MD3 labelled line is probably widespread in the olfactory system of mosquitoes. However, the major challenge to understand such mechanisms in mosquitoes and in insects is our limited odorant screening capabilities. A better understanding of such processes will significantly increase our ability to design potent repellent formulations targeting innate mosquito aversion.

Material and Methods

Insects

Our mosquito colonies were reared in air-controlled insect chambers at 26 ± 2 °C, under a 12 hr:12 hr photoperiod cycle. Larvae were kept in 1 L water-filled plastic containers and fed with a ground mixture of Novocrabs feed (JBL GmbH & Co, Germany). Pupae were transferred into plastic cages until adults emerged. The adults were given 10% sucrose solution *ad libitum*. For oviposition mosquitoes were provided water cup lines with Whatman filter paper. Females were fed with cow blood using a membrane feeding system on days 4 and 5 following adult emergence. *Ae. aegypti* originated from a colony established by Prof. Joel Margalit. The *Ae. aegypti* Liverpool strain was provided by the Akbari lab. *Aedes albopictus* was the FPA Foshan strain collected (Foshan, China) reared at the insectary of the University of Pavia since 2013 (Palatini et al., 2017). *Anopheles gambiae* was the G3 strain originally isolated from West Africa (MacCarthy Island, The Gambia) in 1975 (Federica Bernardini et al., 2017). *Culex pipiens* originated from a wild type population was provided by Dr. Laor Orshan (Ministry of Health, Israel).

Phylogenetic and genomic analyses

The AaegOR49 protein sequence (AAEL001303-PA) was used as a query to identify homologs in other mosquito species. Amino acid sequences of homologous odorant receptors were obtained from the Vectorbase database (vectorbase.org) and the *Tx. amboinensis* genome assembly (Zhou et al., 2014). The multiple sequence alignment was conducted using ClustalW (Chenna et al., 2003). The Maximum-likelihood phylogenetic tree was constructed using MEGAX software (Model: G, bootstraps: 5000). Exon-intron structure analysis was conducted manually by aligning predicted amino-acid sequences to genomic regions. Approximate mapping of the genes in chromosome location for each mosquito species and construction of synteny maps done using Geneious prime software (Kearse et al., 2012) using latest genome assemblies available for each mosquito species (Matthews et al., 2018, Palatini et al., 2020, Boyle et al., 2021, Arensburger et al., 2012, Sharakhova et al., 2007).

Genomic DNA (gDNA) was isolated from whole bodies of *Tx. amboinensis* adults. gDNA was diluted to 25ng/μL in nuclease free water and used as a template in polymerase chain reactions to amplify odorant receptors (TambOR) using Taq polymerase and the following primer sets: TambOr6.F1 (ATGCGCTTCTACGAGAAATAC), TambOr6.R1 (TCAGAAATTATCCTTCAGGATC); TambOr12.F1 (ATGCCATCGGTTTTCTTGGTT), TambOr12.R1 (CTAAAACACTCGCTTCAATATC); TambOr13.F1 (ATGTTCTGCTTCAGGAAGATC), TambOr13.R1 (CTAGAAGTGGTTTTTCAATATAA); TambOr49.F1 (ATGTTGTTCAAGAACTGTTTCC), TambOr49.R1 (TTAATAATTGAATCTTTCCTTCAG); TambOr71.F1 (ATGGGCAGCAGTGATGGTGAC), TambOr71.R1 (CTACTGGTTGATTTTACTGAGG). Cycling conditions were 94°C for 60s; 30 cycles of 94°C for 20s, 56°C for 20s, 72°C for 30s; and a final extension of 72°C for 5 minutes. Amplicons were analyzed by electrophoresis on a 1% agarose gel, cloned into the TOPO-TA

pCR2 plasmid, heat-shock transformed into TOP10 competent *E. coli* cells, and grown overnight at 37°C on LB+ampicillin+X-gal agar plates. Ampicillin resistant, white colonies were isolated using a sterile pipette tip and grown overnight 37°C in 3mL of LB+ampicillin. Plasmids were isolated by DNA miniprep and the Sanger method was used to determine the DNA sequence in both directions using standard T7 and M13.rev primers. TambOR nucleotide sequences were compiled into contigs and intron/exon regions were inferred by comparing to coding sequences described in a previous publication (Zhou et al., 2014).

Chemical reagents

The chemicals used for the deorphanization of receptors were obtained from Acros Organics (Morris, NJ, USA), Alfa Aesar (Ward Hill, MA, USA), ChemSpace (Monmouth Junction, NJ, USA), Sigma Aldrich (St. Louis, MO, USA), TCI America (Portland, OR, USA), and Thermo Fisher Scientific (Waltham, MA, USA) and Penta Manufacturing Corp. (Livingston, NJ, USA) at the highest purity available. *Cannabis* essential oils and sub-mixtures were formulated and supplied by Eybna Technologies (Givat Hen, Israel) (Table S1 and Figure S1).

Two-electrode voltage clamp of Xenopus laevis oocytes

Experimental procedures for *Tx. amboinensis* receptor clones (Table S2) were performed as followed: Stage V-VI *Xenopus laevis* oocytes were harvested, whole ovaries were treated with a 0.8 mg/ml collagenase solution (Sigma Aldrich, 9001-12-1) at 18°C with agitation for 3.5 hours at 60 RPM. Following collagenase treatment, oocytes were washed 5 times in a Ca⁺² free Ringer solution (NaCl 5.61 gr, KCl 0.14 gr, MgCl₂-6 H₂O 0.4 gr, HEPES 1.19 gr, 1L double distilled water [pH 7.6]). Subsequently oocytes were rinsed in a washing solution (96 mM NaCl, 2 mM

KCl, 5 mM MgCl₂ and 5 mM HEPES, 100 µg/mL gentamycin pH 7.6). Finally, oocytes were washed 5 times with incubation medium (96 mM NaCl, 2 mM KCl, 5 mM MgCl₂, 0.8 mM CaCl₂ and 5 mM HEPES, pH 7.6), supplemented with 5% dialyzed horse serum, 50 µg/mL tetracycline, 100 µg/mL streptomycin, and 550 µg/mL sodium pyruvate. Oocytes were allowed to recover overnight prior to injection. Following the night, oocytes were microinjected with 27.6 ng cRNAs, TambOR49 was co-injected with its obligatory co-receptor TambORCO. These genes were not cloned from *Tx. amboinensis* but were custom-synthesized (IDT Coralville, USA) and supplied in a circularized plasmid. The genes were then cloned into *Xenopus* oocytes expression vector pSP64T (DM#111) Addgene (CAT#15030) (Watertown, MA, USA), using Takara-Clontech infusion kit (CAT# 638909). In vitro transcription was done using mMESSAGE Mmachine sp6 Transcription kit (CAT# AM1340) Thermo Fisher (Waltham, MA, USA).

Experimental procedures for *Ae. aegypti*, *Ae. albopictus*, *Cx. pipiens* receptor clones were performed as follows: Stage V-VI *X. laevis* oocytes were ordered from Xenopus1 (Dexter, MI, USA) and incubated in ND96 incubation media (96 mM NaCl, 2mM KCl, 5mM HEPES, 1.8mM CaCl₂, 1mM MgCl₂, pH 7.6) supplemented with 5% dialyzed horse serum, 50 µg/mL tetracycline, 100µg/mL streptomycin, 100µg/mL penicillin, and 550 µg/mL sodium pyruvate. *AaegOr49*, *AaegOrco*, *AalbOr49*, *AalbOrco*, *CquiOr38*, and *CquiOrco* templates were synthesized by Twist Biosciences (San Francisco, CA, USA) and cloned into the pENTRTM vector using the Gateway^R directional cloning system (Invitrogen Corp., Carlsbad, CA, USA) and subcloned into the *X. laevis* expression destination vector pSP64t-RFA. Several of these genes were codon-optimized (Table S2). Plasmids were purified using GeneJET Plasmid Miniprep Kit (ThermoFisher Scientific, Waltham, MA, USA) and sequenced in both directions

to confirm complete coding regions. cRNAs were synthesized from linearized pSP64t expression vectors using the mMESSAGE mMACHINE[®] SP6 kit (Life Technologies). Oocytes were injected with 27.6 nL (27.6 ng of each cRNA) of RNA using the Nanoliter 2010 injector (World Precision Instruments, Inc., Sarasota, FL, USA). Injected oocytes were then incubated at 18°C in 24 well-plates containing 1 ml incubation medium as described above for 3 days prior to recording. OR response was recorded by measuring whole cell currents using the two-electrode voltage clamp (TEVC) method. Holding potential was maintained at −80 mV using an OC-725C oocyte clamp (Warner Instruments, LLC, Hamden, CT, USA). Oocytes were placed in a RC-3Z oocyte recording chamber (Warner Instruments, LLC, Hamden, CT, USA) and exposed for 8-10 s long stimuli. Currents were allowed to return to baseline between odorant applications. Data acquisition was carried out with a Digidata 1550A and pCLAMP10 (Molecular Devices, Sunnyvale, CA, USA). To assess OR activation by ecologically relevant terpenes, selected terpenes were solubilized in 200 µl DMSO prior to dilutions in ND96 buffer supplemented with 0.8 mM CaCl₂. For the initial screen, selected terpenes were used at a concentration of 98 µM and all *Cannabis* essential oils were diluted by a factor of 1.5*10⁵. For CRCs a stock solution of the tested compound was made at concentration of 1M and then further diluted to the desired concentrations.

For pairwise current comparisons of (+)-borneol and (+)-camphor, two separate perfusion systems were assembled, one for each compound. The outlet from each system was connected to a 2 to 1 perfusion manifold. At each tested concentration, (+)-borneol and (+)-camphor were administered consecutively. Oocyte baseline currents were allowed to fully recover between each odorant administration. Each odorant concentration was administered for 8 seconds and the order

of odorant administration was reversed between each tested oocyte to control for any positional effect. Representative current traces can be seen in [Figure S3](#).

Electropalpogram recordings

Based on the voltage clamp data, responses from the maxillary palps of *Ae. albopictus*, *Ae. aegypti*, *Tx. amboinensis*, *Cx. pipiens* and *An. gambiae* were recorded with camphor or borneol. Electropalpogram (EPG) assays were performed according to published procedures (Wang et al., 2017) with a few modifications. Briefly, electrically conductive gel (Parker Laboratories INC, New Jersey, USA) was applied on the metal electrode surface, the head of a 3-6 days old virgin female (not blood-fed) mosquito was cut and mounted on the reference electrode. The distal ends of the maxillary palps were placed on the recording electrode, and the preparation was held using an MP-15 micromanipulator (Syntech GmbH, Germany). EPG signals were acquired by a high-impedance AC/DC IDAC-4 pre-amplifier, and the resulting data were analyzed with EAG Pro version 2.1 software (Syntech GmbH, Germany). A Pasteur pipette was used as a cartridge to deliver the odorant. Within this cartridge, 20 μ L of odorants diluted in hexane were deposited at desired dose onto a 4×20 mm Whatman filter paper strip. The odorants were delivered into a consistent humidified airstream (at a flow rate of 50 cm/s) at approximately 2 cm from the maxillary palps. The pulse duration was 0.1 s, and the recording time was set for 5 s. A 2-min gap was allowed between stimuli to recover the EPG sensitivity. At least 5 individual females were tested, for each individual, 3 technical replicates were performed with doses ranging from 0.01 μ g to 100 μ g. Negative controls (hexane and air) and positive controls (1-octen-3-ol) were performed at both the beginning and end for each recording session to monitor the decline in

sensitivity of the maxillary palps. EPG peak responses were normalized to the response of hexane.

Generating Or49 knockout line in Ae. aegypti and isolating an OR49^{-/-} homozygous line

Genomic DNA was extracted from whole bodies of *Ae. aegypti* Liverpool individuals using the DNeasy Blood & Tissue Kit (Qiagen, Redwood City, CA). Homology arms of the *Or49* gene flanking 1 kb upstream and downstream of the desired insertion site ([Figure S5A](#)) were amplified with the Q5 High Fidelity DNA polymerase (New England Biolabs, Ipswich, MA), using primer pairs Left_Arm_Or49_FWD and Left_Arm_Or49_REV as well as Right_Arm_Or49_FWD and Right_Arm_Or49_REV, respectively ([Table S4](#)). The QF2-ECFP DNA cassette was amplified using the V1117A plasmid as template and the primer pair QF2_OpIE_ECFP FWD and QF2_OpIE_ECFP REV. The cassette contains the *QF2* sequence and the 3' UTR of the *HSP70* gene along with the *ECFP* gene under the control of the *Opie2* promoter and the 3' UTR of the *SV40* gene. PCR bands were cut out from agarose gels and purified with Zymoclean Gel DNA Recovery Kit (Zymo Research, Irvine, CA). Upstream and downstream homology arms as well as the QF2-ECFP cassette PCR products were assembled into the backbone of the V1117A plasmid ([Figure S5B](#)) using Gibson assembly reaction, following the manufacturer recommendations. Gibson's reaction-derived plasmid product was used to transform JM109 cells (Zymo Research), and colonies were individually grown overnight for minipreps with Zyppy Plasmid Miniprep Kit (Zymo Research). The sequence of the plasmid V1117F-Or49 was confirmed by restriction enzyme digestion using the enzymes ScaI-HF and AvrII as well as by whole plasmid sequencing (Primordium Labs, Monrovia, CA). V1117F-Or49 plasmid was used

to retransform JM109 cells, which were grown for maxiprep purification using the PureLink Expi Endotoxin-Free Maxi Plasmid Purification Kit (Thermo Fisher Scientifics, Waltham, MA).

For guide RNA synthesis, non-template reactions were carried out with the gRNA_Left_Or49_F and gRNA_Left_Or49_R forward primers and the universal guide RNA reverse primer (Universal-sgRNA_R). PCR bands were isolated from agarose gel and purified as above described. Guide RNAs were synthesized with the Ambion MEGAscript kit (Thermo Fisher Scientifics) for 4 hours at 37°C, using 300 ng of purified PCR product. Guide RNAs were further purified with the Megaclear Kit (Thermo Fisher Scientifics).

To assess the cleavage activity of the synthesized guide RNAs, *in vitro* Cas9 cleavage assays were carried out. A DNA fragment spanning 1,009 bp overlapping the cleavage sites of the guide RNAs was amplified with primers Or49_cleav_F and Or49_cleav_R, DNA bands were isolated from agarose gel, purified, and 100 ng of which was used in cleavage assays with 300 ng of recombinant Cas9 (PNA BIO, Thousand Oaks, CA) and 100 ng of each guide RNA upon incubation at 37°C for 1 hour (Figure S5C).

For embryo microinjection, an injection mix was prepared with the plasmid V1117F-Or49 at 500 ng/ul, gRNAs left and right at 100 ng/ul each, and recombinant Cas9 at 300 ng/ul. Mix was filtered with the Ultrafree-MC Centrifugal Filter UFC30GUOS (Millipore, Burlington, MA). Freshly harvested *Ae. aegypti* embryos (Liverpool strain) were injected with the transformation mix using a custom-made insect embryo microinjector (Hive Technologies, Cary, NC) at 100 psi pulse and 3 psi back pressures, using quartz needles pulled with a P-2000 needle puller (Sutter Instrument Co., Novato, CA). Genomic DNA of the G1 fluorescent mosquitoes (Figure S5D) were individually extracted with the Qiagen blood kit, and PCR amplified for Sanger Sequencing reactions (Retrogen, San Diego, CA) using the primer pairs Or49_diag_up_F and

Or49_diag_up_R targeting the upstream and primer pair Or49_diag_down_F and Or49_diag_down_R targeting the downstream insertion site (Figure S5E). For whole DNA cassette sequencing (Primordium), 2.5kb DNA fragments were amplified from the DNA of G1 individuals using the primer pair Or49_diag_up_F and Or49_diag_down_R (Figure S5F).

For isolation of homozygous knockout individuals, pupae were sex sorted, and single pairs were transferred into Narrow *Drosophila* Vials (Genesee Scientific, El Cajon, CA), filled with 10 mL of deionized water (DI) and closed with cotton stoppers. Upon emergence, water was drained, and sugar cottons were placed into the vials. Mosquitoes were allowed to mate for 5 days in the vials, and then all individuals were transferred to a single cage for blood feeding. Three days after blood feeding, females were individually transferred to a fresh vial containing a piece of brown paper towel wetted with 1 mL DI water. Females were allowed to lay eggs, and each egg batch was individually hatched in 250 mL Clear Pet Cups (9oz). Larvae were screened for fluorescence, and the batches that resulted in 100% fluorescent individuals were grown to adulthood and intercrossed to confirm homozygosity in the following generation. Two out of thirty egg batches resulted in homozygous offspring. To further confirm the homozygous status of these individuals, genomic DNA of three pools of 10 males, 10 females, and a mix of males and females were PCR amplified with the primer pair Or49_diag_up_F and Or49_diag_down_R, which resulted in a single band for homozygous individuals and two bands for heterozygous individuals (Figure S5G).

Single-sensillum electrophysiology

Single sensillum recordings from capitate peg sensilla on the maxillary palp of wild type *Ae. aegypti* (Liverpool), *Ae. albopictus* (FPA), *Cx. quinquefasciatus* (Thai) and *An. gambiae sensu*

stricto (G3) and *Ae. aegypti* *Or49^{-/-}* mutant mosquitoes were performed using an established protocol (Herre et al., 2022). Briefly, a single cold-anesthetized female mosquito was placed ventrally on a microscope slide, which was covered with a double-sided sticky tape. Another piece of tape was placed on top of the dorsal side of the body and then pushed against the underlying tape to keep the insect from moving. The maxillary palps were then gently mounted on a piece of double-sided tape. Thereafter, the specimen was placed under a light microscope (700× magnification) to visualize the capitae peg sensilla for extracellular recordings.

Two tungsten microelectrodes were electrolytically sharpened and mounted in holders (Ockenfels Syntech GmbH, Buchenbach, Germany). The ground electrode was placed in the eye of the mosquito, while the recording electrode, which was attached to a high-impedance universal single ended probe (Ockenfels Syntech GmbH), was introduced into a sensillum with a piezo-controlled micro manipulator until electrical contact was achieved. Signals were routed to an Intelligent Data Acquisition Controller (Ockenfels Syntech GmbH), and were visualized on a computer screen. Spikes were quantified offline using the established nomenclature for the sensory neurons (Ghaninia et al., 2019). The number of spikes counted during a 0.5 s stimulus delivery interval was subtracted from the number of spikes counted during a 0.5 s prestimulus period, and the result was multiplied by 2 to obtain the activity of individual sensory neurons housed in the capitae peg sensillum as a spikes/s measurement.

To investigate the physiological activity of the A, B and C neurons housed in single capitae peg sensilla, CO₂, *R*-(-)-1-octen-3-ol and (+)-borneol were used: gas cylinders containing metered amounts of CO₂ (300, 600, 1200, 2400, or 4800 ppm) and oxygen (20%), balanced by nitrogen (Strandmöllen AB, Ljungby, Sweden) were used to assess the activity of the A neuron; serial decadic dilutions of *R*-(-)-1-octen-3-ol (CAS: 3687-48-7, Penta Manufacturing, Livingston,

USA), diluted in paraffin oil, were used to assess the activity of the B neuron; and serial decadic dilutions of (+)-borneol (CAS: 464-43-7, Sigma-Aldrich, St. Louis, MO, USA), diluted in diethyl ether (SupraSolv, Billerica, MA, USA) were used to assess the activity of the C neuron. Pasteur pipettes were filled with the metered CO₂ and used immediately to stimulate the preparation. A 15 µL aliquot of each dilution of *R*-(-)-1-octen-3-ol and (+)-borneol was pipetted onto a filter paper (5 mm × 15 mm) inserted inside a Pasteur pipette, and the diethyl ether was allowed 15 min to evaporate, before being used for stimulus delivery. All stimuli were delivered into the airstream passing over the maxillary palp preparation.

Calcium imaging in the Ae. aegypti antennal lobe (AL)

Odor-evoked responses in the *Ae. aegypti* antennal lobe (AL) were imaged using the *brp-QF2>QUAS-GCaMP6s* progeny from the *brp-QF2* and *QUAS-GCaMP6s* parental lines (Zhao et al., 2022). A total of eight 6-8 day-old female mosquitoes were used for all calcium experiments. Each mosquito was cooled on ice and transferred to a Peltier-cooled holder that allowed the mosquito head to be fixed to a custom stage using ultraviolet glue. The stage permits the superfusion of saline to the head capsule and space for wing and proboscis movement (Lahondère et al., 2019; Melo et al., 2020). Once the mosquito was fixed to the stage, a window in its head was cut to expose the brain, and the brain was continuously superfused with physiological saline (Vinauger et al., 2019). Calcium-evoked responses in the AL were imaged using the Prairie Ultima IV two-photon excitation microscope (Prairie Technologies) and Ti:Sapphire laser (Chameleon Ultra; Coherent; at 1910 mW power). Experiments were performed at 75 µm depth from the ventral surface of the AL, allowing characterization of the mediodorsal glomerular responses to olfactory stimuli and allowing these glomeruli to be repeatedly imaged

across preparations. To record odor-evoked responses, images were collected from a $110\ \mu\text{m} \times 83\ \mu\text{m}$ plane at 2 Hz (line period of 1 ms), and for each odor stimulus, images were acquired for 25 s, starting 10 s before the stimulus onset. Image data were imported into Matlab (v2017; Mathworks, Natick, Massachusetts) for Gaussian filtering (2×2 pixel; $\sigma = 1.5$ -3) and alignment using a single frame as the reference at a given imaging depth and subsequently registered to every frame to within $\frac{1}{4}$ pixel. Odor stimuli were diluted to 10^{-3} and 10^{-4} concentration in hexane (>99.5% purity; Sigma), with hexane used as the solvent control. During an experiment, odor stimuli were separated by intervals of 120 s to avoid receptor adaptation, and odor syringes were used once per preparation to prevent decreased concentration within the cartridge. Calcium responses are calculated as the change in fluorescence and time-stamped and synced with the stimulus pulses. After an experiment, the AL was sequentially scanned at $0.5\ \mu\text{m}$ depths from the ventral to the dorsal surface to provide glomerular assignment and registration between preparations. Glomeruli ($1\ \mu\text{m}^3$ voxel) were mapped and registered based on the positions and odor-evoked responses of the putative AL3, MD1-3, and AM2 glomeruli, using available AL atlases (Shankar and McMeniman, 2020; Wolff et al., 2023) and the Amira software (v. 6.5, FEI Houston Inc.).

Behavioral assay

The role of borneol in human host-seeking female mosquitoes was examined with an arm-in-a-cage assay described previously (Dekel et al., 2022) with minor modifications ([Additional File 1A](#)) in an air-conditioned room ($26 \pm 1\ ^\circ\text{C}$, $60 \pm 5\ \%$ RH). Briefly, the experimenter's hand was presented to fifteen 5–10 days post emergence adult females. A three-dimensional-printed interlocking ring with a diameter of 55 mm was used in this experiment ([Additional File 1B](#)).

The ring was placed over the dorsal side of a nitrile glove (powder-free latex). To evoke human odor and prevent mosquito bites, we replaced the nitrile between the two ring components with a plastic screen. The interlocking ring included a central odorant delivery platform ([Additional File 1C](#)) comprising a 10-mm-diameter cover glass and two 5-mm-diameter filter discs (WHA10016508; Merck) for the evaluation of VOCs that interact with or blend with human odor (stl files are provided in [additional files 2 and 3](#)). Plastic screen, nitrile glove and odorant delivery platform were replaced between repetitions to avoid contaminations. Mosquitoes were placed in a 20.3-cm³ metal cage located in an experimental room with a vent, under a video camera (EOS 70D, lens: MACRO 0.25/0.8ft; Canon Inc., Tokyo, Japan) and a light ring. Mosquitoes were allowed to acclimate for ten minutes before recording. Mosquito behavior was recorded for 10 min at 25 frames per second. The number of mosquito detection on the screen and ring were automatically counted using a custom YOLOv5 model (see object detection section below). The possible number of detections per experiment was calculated as 225,000, obtained by multiplying the number of mosquitoes in the cage (15) by the frame rate (25 frames per second) and the duration of each experiment (600 seconds). We used the solvent diethyl ether (DEE) as a vehicle. On a blank filter disc, 25 μ L of DEE, and DEE with racemic borneol (1M, 3.58 mg) were deposited on the filter paper and allowed to evaporate for 2 min prior to mosquito exposure outside the experimental room to avoid contamination. To enhance attractiveness, at the beginning of each experiment, the experimenter first rubbed the ring-mounted glove against the shirt and skin for 1 minute. Additionally, the experimenter blew twice, once into the cage and once into the glove. All experiments were conducted during the first 4 hours of the diurnal period and lasted 10 min. This schedule was chosen for practical reasons and because mosquitoes consistently exhibited attraction to the human hand. Mosquito detection was normalized to the

mean detection of the control $\left(\frac{\text{detections for minute } i}{\text{mean detection for all minutes (control)}} * 100 \right)$. Statistical comparisons of mosquito detections per minute were carried out with Mann Whitney U test (P -value < 0.001 , $n = 3$). For data variation across time and repetitions, see [Figure S7](#). Data was analyzed using R Studio (Team, 2021) The R-code and behavioral data can be found in [additional files 4-6](#).

YOLOv5 Model Training and Custom Dataset

In this study, we trained the YOLOv5l model using a customized dataset comprising images from the bioassay, along with additional data from previously published literature (Janson et al., 2023), to investigate the ecological role of borneol on mosquitoes. The training process involved 100 epochs with a batch size of 32, utilizing separate sets of images and corresponding annotations for training, validation, and testing (4,759, 1,584, and 1,580 images, respectively). To assess the model's performance, we employed the mean Average Precision (mAP) metric across a range of intersection-over-union (IoU) thresholds from 50% to 95% (mAP50-95). The resulting mAP50-95 value of 0.662 indicates the average precision considering different IoU thresholds. At a 50% IoU threshold, the mAP50 was measured as 0.982, demonstrating high accuracy in detection. Furthermore, the recall value of 0.969 indicates a high proportion of true positive detections, while the precision value of 0.974 reflects accurate identification of mosquitoes. It's worth noting that detections were collected with a minimum confidence threshold of 0.5 to ensure reliable results. Video samples with automated detection are available in [additional file 8](#).

Figure legends

Figure 1. The phylogenetically-conserved gene encoding OR49. **A)** Amino-acid sequence alignment of OR49 homologs in *Culex quinquefasciatus* (Cqui), *Aedes albopictus* (Aalb), *Aedes aegypti* (Aaeg), *Toxorhynchites amboinensis* (Tamb), and *Anopheles gambiae* (Agam). The top chart presents the amino-acid consensus. High consensus marked in green to yellow, low consensus are in red. **B)** Amino-acid sequence identity matrix. Intensity of shading indicates percentage of homologies. **C)** Phylogenetic tree of mosquito OR49 proteins (green). Closest brachyceran homologs (red branches) include *Glossina fuscipes* (Gfuc) and *Drosophila melanogaster* (Dmel). Bootstrap support above 50% are shown. Gene exon structure of OR49 genes and other phylogenetically-related genes. **D)** Exon composition of the OR49 group and related homologs. Exons are labeled in white and black. The nucleotide positions of exon-exon boundaries are shown and intron phases are color-coded. **E)** Chromosomic locations of Or49 homolog genes (green) and indolergic ORs (indolORs, in red). **F)** Syntenic relationships of OR49 genes in mosquito species and gene structure of OR49 genes.

Figure 2. Odorant receptor 49 is a borneol receptor. **A)** The 4th segment of the mosquito maxillary palps houses three neurons, including the CO₂ capitate-peg neuron (cpA) expressing three gustatory receptors, the 1-octen-3-ol-sensitive neuron (cpB), and the orphan neuron (cpC). **B)** The response profile of *Aedes albopictus* OR49 (AalbOR49) in response to odorant mixtures (100 µM) belonging to a variety of chemical classes highlights the activity of ketones. Terpenoids, including camphor and fenchone are the most efficacious activators of AalbOR49. Bicyclic monoterpenoids are labeled in green. Statistical differences were evaluated by ANOVA followed by a Kruskal-Wallis multiple comparisons test. ns, non-significant, *p < 0.0332, **p < 0.0021, ***p < 0.0002 and ****p < 0.0001. Data indicate the means ± SEM. **C)** Pineapple Haze

(PH), OG Kush (OGK), Adom9 (A9), and Master Kush (MK) elicited the highest currents from *Toxorhynchites amboinensis* OR49 (TambOR49). Borneol content is indicated on the right Y-axis. **D)** Response of TambOR49 to 6 *Cannabis* sub-mixtures and the constituents from sub-mixture 2. **E)** Concentration-response relationships of TambOR49 to the two borneol enantiomers. **F)** Concentration-response relationships of TambOR49, *Culex quinquefasciatus* OR38 (CquiOR38), *Ae. aegypti* OR49 (AaegOR49) and AalbOR49 in response to (+)-borneol and (+)-camphor. Effective concentrations at 50% of the maximal response (EC_{50}) are circled. **G)** Pairwise comparisons of the current responses of all four mosquito species OR49s elicited by increasing concentrations of (+)-borneol and (+)-camphor. Statistical differences were evaluated by multiple t-tests. * $p < 0.0332$, ** $p < 0.0021$, *** $p < 0.0002$ and **** $p < 0.0001$. Data indicate the means \pm SEM. Representative current traces can be found in [Figure S3](#).

Figure 3. The maxillary palp of culicine mosquitoes respond to borneol and camphor. A) Electropalpogram (EPG) responses in *Aedes albopictus*, *Aedes aegypti*, *Culex pipiens*, and *Anopheles gambiae*. EPG responses to 1-octen-3-ol (blue, 10 μ g), camphor (purple, 10 μ g), and borneol (green, 10 μ g) enantiomers relative to hexane. Representative traces for each odorant are shown below the x-axis. Statistical differences were evaluated via one-way anova. * $p < 0.05$, ** $p < 0.01$, *** $p < 0.005$ and **** $p < 0.001$. Data indicate the means \pm SEM, $n = 15$. **B)** Dose-response relationships of the maxillary palps of three culicine mosquito species in response to increasing concentrations of (+)-borneol and (+)-camphor. Representative traces are shown on the right. Statistical differences were evaluated by multiple t-tests. Data indicate the means \pm SEM, $n = 15$.

Figure 4. Species-dependent response to (+)-borneol of the C neuron of the capitae peg sensilla and its reliance of *Or49* in *Ae. aegypti*. **A)** A tungsten electrode was used to record action potentials (spikes) from the capitae peg sensillum on the maxillary palp, which houses three neurons. The cpA neuron responds to CO₂ (large spike in traces), the cpB neuron responds to 1-octen-3-ol (medium size spikes) and the cpC neuron responds to borneol (small size spikes). **B)** Species- and dose-dependent response of the C neuron to (+)-borneol with mean \pm s.e.m. at each concentration. The arrow and dotted line indicate the borneol dose to the shown representative traces. *Ae. aegypti* ($n = 10$), *Ae. albopictus* ($n = 7$), *Cx. quinquefasciatus* ($n = 2$), *Ae. aegypti Or49^{-/-}* ($n = 8$), *An. gambiae* ($n = 15$). Representative traces of the cp sensilla of *Ae. albopictus* and *Cx. quinquefasciatus* are available in [Figure S6](#). **C-D)** The spontaneous activity of the three sensory neurons in the capitae peg sensilla of *Ae. aegypti* and *Anopheles gambiae* s.s.. In the top traces, note the differences in spike amplitude of the A, B (orange markers) and C neurons (green markers). **C)** *R*-(–)-1-octen-3-ol and (+)-borneol elicit responses in the B and C neurons of *Ae. aegypti*, respectively. The response to (+)-borneol is abolished in *Or49^{-/-}* mutant mosquitoes. **D)** The C neuron of *An. gambiae* s.s. does not respond to (+)-borneol.

Figure 5. Borneol elicits robust responses in the *Ae. aegypti* AL. **A)** Schematic of the two-photon setup used to record calcium dynamics in the mosquito antennal lobe (AL). **B)** AL atlas, highlighting the MD1 (blue), MD2 (orange), and MD3 (green) glomeruli. Non-responsive AL glomeruli (grey) and the mediodorsal glomeruli were registered and mapped to previously published atlases. **C)** Pseudo color plot from a single preparation of $\Delta F/F_0$ calcium responses (0-0.8 scale) to (+)-borneol (10^{-4} dilution), at a depth of 75 μ m from the surface of the AL. Borneol evoked a strong response in the region of interest mapped to the MD3 glomerulus (highlighted in

white). **D)** Glomerular responses ($\Delta F/F_0$) to (+)-borneol for the MD1, MD2, and MD3 glomeruli. Lines are the mean of one glomerulus ($n = 4-8$ preparations); shaded areas are the SEM. The grey bar denotes stimulus duration (2 s). **E)** Same as in D, except the glomeruli were stimulated with 1-octen-3-ol (10^{-4} dilution). **F)** Same as in D, except the glomeruli were stimulated with CO_2 (5%). **(G)** Tuning curve for the MD3 glomerulus to a limited panel of 8 odorants, each tested at 10^{-4} concentration. The MD3 glomerulus (bars in green) showed significant calcium responses to enantiomers of borneol and camphor compared to the solvent control (Kruskal-Wallis test: $\chi^2 = 37.1$, $P < 0.0001$; posthoc multiple comparisons: $p < 0.05$). Bars represent the mean \pm SEM.

Figure 6. Borneol inhibits host-seeking female *Ae. aegypti* (Liverpool) behavior. Average number of mosquito detections per minute (normalized to the control group) in the region of interest (ROI) in response to control (DEE) and treatment (DEE + racemic borneol). Mosquito detection on the ROI was normalized to the control. The statistical comparison involved analyzing 30 data points of accumulative detections per minute for each treatment. The data was analyzed with Pairwise comparisons using Wilcoxon rank sum test ($p\text{-value} < 0.001$, $n = 3$). **B)** A representative of the number of mosquitoes detected in the ROI as a function of time is shown on the right side of each treatment (right y-axis).

Supplementary information

Figure S1. List of volatile organic compounds present in *Cannabis* essential oils. Each Cannabis blend represented by a distinct color is composed of VOCs belonging mainly to different terpene categories but also to non-terpene chemical classes.

Figure S2. VOC content in *Cannabis* essential oils.

Figure S3. Representative current traces of mosquito OR49 proteins. A) Representative traces of TambOR49+TambOrco injected oocytes vs monoterpene blends and compounds. Pineapple Haze (PH), Adom #9 (A9), O.G Kush (OGK), Master Kush (MK) and Jack Herrer (JH) triggered a measurable response. (±)-camphor, (+)-camphor, (+)-fenchone and eucalyptol were used as positive controls at concentration of 0.1 mM, all *Cannabis* essential oils were diluted by a factor of 1.5×10^5 . B) Representative trace of TambOR49+TambOrco vs sub-mixtures No. 1 through 6, which were formulated based on overlapping active compounds from *Cannabis* essential oils. All sub-mixtures were diluted by a factor of 1.5×10^6 . Only sub-mixture No.2 activated TambOR49+TambOrco. (+)-Camphor was used as positive control at concentration of 0.1 mM. C) Representative trace of TambOR49+TambOrco vs the components of sub-mixture No. 2. (±)-Borneol elicited currents 8-fold larger than the other tested single monoterpenoids. All compounds were tested at concentration of 0.1 mM. D) Representative traces of TambOR49+TambOrco concentration response curves (CRCs). Top left TambOR49+TambOrco vs (-)-borneol, Top right TambOR49+TambOrco vs (+)-borneol and bottom left TambOR49+TambOrco vs (+)-camphor. E) Representative traces of AegOR49 CRC's. Left AegOR49 vs (-)-Borneol; right, AegOR49 vs (+)-Borneol. F) Representative traces of CquiOR38+CquiOrco CRCs in response to increasing concentrations of (+)-camphor (left) and (+)-borneol (right). G) Representative traces of AegOR49+Orco CRCs in response to increasing concentrations of (+)-camphor (left) and (+)-borneol (right). H) Representative traces of AalbOR49+AalbOrco CRCs in response to increasing concentrations of (+)-camphor (left)

and (+)-borneol (right). **I)** Representative traces of pairwise current comparisons between (+)-camphor and (+)-borneol. From top to bottom, TambOR49+TambOrco, CquiOR38+CquiOrco, AaegOR49+AaegOrco and AalbOR49+AalbOrco. Down arrows indicate odorant administrations and concentrations. All concentrations are in micromolar [μ M].

Figure S4. *Anopheles gambiae* OR28 (AgamOR28) does not respond to borneol. **A)** Concentration-response of AgamOR28 in response to increasing concentrations of four plant volatile organic compounds, including aromatic (acetophenone and α -terpineol) and terpenoid compounds (α -pinene and (+)-borneol). EC₅₀ values shown in the inset are in the low millimolar range. **B)** Representative current traces of AgamOR28-Orco activation by 4 plant volatile organic compounds. Arrowheads above the traces indicate the onset of the odorant stimulus.

Figure S5. Construction of *Ae. aegypti* Or49 knockout line. **A)** Diagram depicting the *Ae. aegypti* Or49 gene and the gRNA target sites on the top and the insertion cassette on the bottom flanked by the upstream (Left) and downstream (Right) homology arms. The insertion cassette encompasses the *QF2* sequence and the 3' UTR of the *HSP70* gene along with the *ECFP* gene under the control of the *Opie2* promoter and the 3' UTR of the *SV40* gene. Arrows indicate primer binding sites. Primers P1-12 are listed in Table S4. **B)** Plasmid V1117F-Or49 map. **C)** *In vitro* Cas9 cleavage assay. Guide RNAs left and right targeting the Or49 gene almost completely digested PCR fragment containing target sequence. (–) negative controls without guide RNAs show no PCR fragment digestion. **D)** Sanger sequencing of amplified PCR fragments of G1 transgenic male individuals unveiling the sequences overlapping upstream (left) and downstream (right) of the DNA cassette inserted by homology directed repair. **E).** Sequencing of G1

individuals showing the complete insertion of the DNA cassette containing *QF2* and *ECFP*. The presence of a single point mutation was confirmed as an artifact and excluded by Sanger sequencing. F) Diagnostic PCR reactions showing the presence of double bands in single G1 heterozygous individuals and single upper band in pools of 10 individuals of the *OR49*^{-/-} homozygous line.

Figure S6. Response to (+)-borneol of the cpC neuron of the capitae peg sensilla of *Ae. aegypti* and *Cx. quinquefasciatus*. Representative SSR traces from the *Ae. albopictus* and *Cx. quinquefasciatus* cp sensilla stimulated with 0.01% (+)-borneol. Note the differences in spike amplitude of the A, B (orange markers) and C neurons (green markers).

Figure S7. Behavior replicates. Detection variations in control and borneol treatments. A) Replicate behavioral experiments with the arm-in-a-cage assay. **B)** Box plot showing the detection variation of each experimental replicate in the control and borneol treatments. The y-axis represents the number of mosquito detections per minute over a 10-minute period. The x-axis indicates the replicate. Number. **C)** Accumulative detections over time. The y-axis represents the accumulative number of mosquito detection per minute.

Table S1. List of blends and single compounds used in the pharmacological screen.

Table S2. List of *Or* genes.

Table S3. Raw pharmacological data.

Table S4. Primer list (*Or49* knockout).

Additional File 1: Diagrams of the odor delivery system. The odor delivery system is composed of interlocking top and bottom rings attached to a removable chemical holder (overview, top, bottom and side views are provided). Dimensions are provided in millimeters.

Additional file 2: Hand rings.stl. File format for 3D-printing of the two complementary hand rings.

Additional file 3: Chemical holder.stl. File format for 3D-printing of the chemical holder component.

Additional file 4: Behavioral data. CSV file of collected mosquito visits on the ROI.

Additional file 5 and 6: Codes for analyzing behavioral data. R file to analyze the data and generate figure 6 (arm-in-a-cage_with_yolov5.R) and S5 (Supplementary_plot.R). Post-processing was carried out using Adobe Illustrator.

Additional file 7. Video recording example of the of the female *Ae. aegypti* antennal lobe.

Additional file 8. Video recording example of the arm-in-a-cage assay. Thirty-second-long recording example at the 4-minute mark of mosquito landing behavior in the presence of the vehicle diethyl ether (DEE) and racemic borneol.

Authors contributions

RJP initiated the functional characterization of OR49. JB conceived the study. YV identified borneol as a key OR49 ligand. YW conducted mosquito electropalpograms. RMH identified camphor as an OR49 agonist. OSA and IVC-A engineered the *Ae. aegypti* Or49 knockout strain. MG and RI designed and conducted the single sensillum recordings. ESS conducted the behavioral experiments. DP and PP conducted gene annotations, phylogenetic analyses and described OR49 syntenic relationships. DR completed the *Toxorhynchites amboinensis* OR

genomic PCRs and sequencing. EY provided genetic constructs and injectable mRNA. AW provided funding and scientific oversight. JB wrote the manuscript with individual contributions from all the authors.

Acknowledgements

We thank Ziv Kassner for consultation, processing and analysis guidance, and technical support in the creation of the mosquito detection model. We are especially grateful to Nadav Eyal at Eybna Terpene Based Technologies for their time and supply of *Cannabis* essential oils. We are grateful to Dr. Laor Orshan (Ministry of Health, Israel) for providing a colony of *Culex pipiens*. Dr. Pitts and Bohbot are co-corresponding authors.

References

- Abdelgaleil, S.A.M., Al-Nagar, N.M.A., Abou-Taleb, H.K., Shawir, M.S., 2022. Effect of monoterpenes, phenylpropenes and sesquiterpenes on development, fecundity and fertility of *Spodoptera littoralis* (Boisduval). *Int. J. Trop. Insect Sci.* 42, 245–253. <https://doi.org/10.1007/s42690-021-00539-y>
- Abdelgaleil, S.A.M., Mohamed, M.I.E., Badawy, M.E.I., El-arami, S.A.A., 2009. Fumigant and contact toxicities of monoterpenes to *Sitophilus oryzae* (L.) and *Tribolium castaneum* (Herbst) and their inhibitory effects on acetylcholinesterase activity. *J. Chem. Ecol.* 35, 518–525. <https://doi.org/10.1007/s10886-009-9635-3>
- Afify, A., Galizia, C.G., 2014. Gravid females of the mosquito *Aedes aegypti* avoid oviposition on m-cresol in the presence of the deterrent isomer p-cresol. *Parasite Vector* 7, 315. <https://doi.org/10.1186/1756-3305-7-315>
- Alavez-Rosas, D., Socorro-Benitez, C., Cruz-Esteban, S., 2022. Repellent and adulticidal effect of essential oils mixtures on *Aedes aegypti* females. *Int J Trop Insect Sc* 42, 1885–1892. <https://doi.org/10.1007/s42690-021-00716-z>
- Amer, A., Mehlhorn, H., 2006. Repellency effect of forty-one essential oils against *Aedes*, *Anopheles*, and *Culex* mosquitoes. *Parasitol Res* 99, 478–490. <https://doi.org/10.1007/s00436-006-0184-1>

- 859 Andreazza, F., Valbon, W., Dong, K., 2023. Transfluthrin enhances odorant receptor-mediated
860 spatial repellency in *Aedes aegypti*. Pestic Biochem Phys 192, 105387.
861 <https://doi.org/10.1016/j.pestbp.2023.105387>
- 862 Anton, S., Loon, J. van, Meijerink, J., Smid, H., 2003. Central projections of olfactory receptor
863 neurons from single antennal and palpal sensilla in mosquitoes. Arthropod Structure &
864 Development 32, 319-327. <https://doi.org/10.1016/j.asd.2003.09.002>
- 865 Baker, M., 1996. Fur rubbing: Use of medicinal plants by capuchin monkeys (*Cebus capucinus*).
866 Am. J. Primatol. 38, 263–270. [https://doi.org/10.1002/\(sici\)1098-2345\(1996\)38:3<263::aid-ajp5>3.0.co;2-x](https://doi.org/10.1002/(sici)1098-2345(1996)38:3<263::aid-ajp5>3.0.co;2-x)
- 868 Benelli, G., Flamini, G., Fiore, G., Cioni, P.L., Conti, B., 2013. Larvicidal and repellent activity
869 of the essential oil of *Coriandrum sativum* L. (Apiaceae) fruits against the filariasis vector
870 *Aedes albopictus* Skuse (Diptera: Culicidae). Parasitol Res 112, 1155–1161.
871 <https://doi.org/10.1007/s00436-012-3246-6>
- 872 Bohbot, J., Pitts, R.J., Kwon, H.W., Rutzler, M., Robertson, H.M., Zwiebel, L.J., 2007.
873 Molecular characterization of the *Aedes aegypti* odorant receptor gene family. Insect
874 molecular biology 16, 525–537. <https://doi.org/10.1111/j.1365-2583.2007.00748.x>
- 875 Bohbot, J.D., Dickens, J.C., 2010. Insect repellents: modulators of mosquito odorant receptor
876 activity. PLoS ONE 5, e12138. <https://doi.org/10.1371/journal.pone.0012138>
- 877 Bohbot, J.D., Fu, L., LE, T.C., Chauhan, K.R., Cantrell, C.L., Dickens, J.C., 2011. Multiple
878 activities of insect repellents on odorant receptors in mosquitoes. Medical and veterinary
879 entomology 25, 436–444. <https://doi.org/10.1111/j.1365-2915.2011.00949.x>
- 880 Carey, A.F., Wang, G., Su, C.-Y., Zwiebel, L.J., Carlson, J.R., 2010. Odorant reception in the
881 malaria mosquito *Anopheles gambiae*. Nature 464, 66–71.
882 <https://doi.org/10.1038/nature08834>
- 883 Cloyd, R.A., Marley, K.A., Larson, R.A., Dickinson, A., Arieli, B., 2011. Repellency of
884 naturally occurring volatile alcohols to fungus gnat *Bradysia* sp. nr. *coprophila* (Diptera:
885 Sciaridae) adults under laboratory conditions. J Econ Entomol 104, 1633–1639.
886 <https://doi.org/10.1603/ec11066>
- 887 Conti, B., Benelli, G., Leonardi, M., Afifi, F.U., Cervelli, C., Profeti, R., Pistelli, L., Canale, A.,
888 2012. Repellent effect of *Salvia dorisiana*, *S. longifolia*, and *S. sclarea* (Lamiaceae) essential
889 oils against the mosquito *Aedes albopictus* Skuse (Diptera: Culicidae). Parasitol Res 111,
890 291–299. <https://doi.org/10.1007/s00436-012-2837-6>
- 891 Dayaram, L., Khan, A., 2016. Repellent, fumigant and contact toxicity of *Salvia officinalis*,
892 *Rosmarinus officinalis* and *Coriandrum sativum* against *Callosobruchus maculatus* (Fab.)
893 (Coleoptera:Bruchidae). NAAS 34, 893–902.

- 894 Dekel, A., Sar-Shalom, E., Vainer, Y., Yakir, E., Bohbot, J.D., 2022. The oviposition cue indole
895 inhibits animal host attraction in *Aedes aegypti* (Diptera: Culicidae) mosquitoes. Parasite
896 Vector 15, 422. <https://doi.org/10.1186/s13071-022-05545-8>
- 897 Dekel, A., Yakir, E., Bohbot, J.D., 2019. The sulcatone receptor of the strict nectar-feeding
898 mosquito *Toxorhynchites amboinensis*. Insect Biochemistry and Molecular Biology 111,
899 103174. <https://doi.org/10.1016/j.ibmb.2019.05.009>
- 900 Dickens, J.C., Bohbot, J.D., 2013. Mini Review: Mode of action of mosquito repellents.
901 Pesticide Biochemistry and Physiology 106. 149–155.
- 902 Drapeau, J., Fröhler, C., Touraud, D., 2009. Repellent studies with *Aedes aegypti* mosquitoes and
903 human olfactory tests on 19 essential oils from Corsica, France. Flavour and Fragrance
904 Journal 24, 160-169. <https://doi.org/10.1002/ffj.1928>
- 905 Enan, E., 2001. Insecticidal activity of essential oils: octopaminergic sites of action. Comp.
906 Biochem. Physiol. Part C: Toxicol. Pharmacol. 130, 325–337. [https://doi.org/10.1016/s1532-0456\(01\)00255-1](https://doi.org/10.1016/s1532-0456(01)00255-1)
- 908 Erdelyan, C.N.G., Mahood, T.H., Bader T.S.Y., Whyard, S. 2011. Functional validation of the
909 carbon dioxide receptor genes in *Aedes aegypti* mosquitoes using RNA interference. Insect
910 molecular biology 21, 119-127. <https://doi.org/10.1111/j.1365-2583.2011.01120.x>
- 911 Ghaninia, M., Majeed, S., Dekker, T., Hill, S.R., Ignell, R., 2019. Hold your breath – Differential
912 behavioral and sensory acuity of mosquitoes to acetone and carbon dioxide. Plos One 14,
913 e0226815. <https://doi.org/10.1371/journal.pone.0226815>
- 914 Gillies, M.T., 1980. The role of carbon dioxide in host-finding by mosquitoes (Diptera:
915 Culicidae): a review. Bull Entomol Res 70, 525–532.
- 916 Gordon, U., Ruther, J., Bernier, U.R., Rose, A., Geier, M., 2018. Development and evaluation of
917 push-pull control strategies against *Aedes aegypti* (Diptera: Culicidae), in: Norris, E.J., Coats,
918 J.R., Gross, A.D., Clark, J.M. (Eds.), Advances in the Biorational Control of Medical and
919 Veterinary Pests. ACS Publications, pp. 187–204. <https://doi.org/10.1021/bk-2018-1289.ch010>
- 921 Grant, A.J., Dickens, J.C., 2011. Functional characterization of the octenol receptor neuron on
922 the maxillary palps of the yellow fever mosquito, *Aedes aegypti*. PLoS ONE 6, e21785.
923 <https://doi.org/10.1371/journal.pone.0021785>
- 924 Grant, A.J., O'Connell, R.J., 1996. Electrophysiological responses from receptor neurons in
925 mosquito maxillary palp sensilla., in: Block, E. (Ed.), Ciba Found Symp. John Wiley & Sons,
926 Ltd., pp. 233-48-discussion 248-53-281–4.
- 927 Herre, M., Goldman, O.V., Lu, T.-C., Caballero-Vidal, G., Qi, Y., Gilbert, Z.N., Gong, Z.,
928 Morita, T., Rahiel, S., Ghaninia, M., Ignell, R., Matthews, B.J., Li, H., Vosshall, L.B.,

- 929 Younger, M.A., 2022. Non-canonical odor coding in the mosquito. *Cell* 185, 3104-3123.e28.
930 <https://doi.org/10.1016/j.cell.2022.07.024>
- 931 Hill, C.A., Fox, A.N., Pitts, R.J., Kent, L.B., Tan, P.L., Chrystal, M.A., Cravchik, A., Collins,
932 F.H., Robertson, H.M., Zwiebel, L.J., 2002. G protein-coupled receptors in *Anopheles*
933 *gambiae*. *Science* (New York, NY) 298, 176–178. <https://doi.org/10.1126/science.1076196>
- 934 Höld, K.M., Sirisoma, N.S., Ikeda, T., Narahashi, T., Casida, J.E., 2000. α -Thujone (the active
935 component of absinthe): γ -Aminobutyric acid type A receptor modulation and metabolic
936 detoxification. *Proc. Natl. Acad. Sci.* 97, 3826–3831. <https://doi.org/10.1073/pnas.070042397>
- 937 Hwang, Y.-S., Wu, K.-H., Kumamoto, J., Axelrod, H., Mulla, M.S., 1985. Isolation and
938 identification of mosquito repellents in *Artemisia vulgaris*. *J Chem Ecol* 11, 1297–1306.
939 <https://doi.org/10.1007/bf01024117>
- 940 Iovinella, I., Pelosi, P., Conti, B., 2014. A rationale to design longer lasting mosquito repellents.
941 *Parasitology research* 113, 1813–1820. <https://doi.org/10.1007/s00436-014-3827-7>
- 942 Janson, K.D., Carter, B.H., Jameson, S.B., Verges, J.E. de, Dalliance, E.S., Royse, M.K., Kim,
943 P., Wesson, D.M., Veishe, O., 2023. Development of an automated biomaterial platform to
944 study mosquito feeding behavior. *Frontiers Bioeng Biotechnology* 11, 1103748.
945 <https://doi.org/10.3389/fbioe.2023.1103748>
- 946 Jocher, G., Chaurasia, A., Stoken, A., Borovec, J., NanoCode012, Kwon, Y., Michael, K.,
947 TaoXie, Fang, J., imyhxy, Lorna, Yifu, zeng, Wong, C., V, A., Montes, D., Wang, Z., Fati,
948 C., Nadar, J., Laughing, UnglvKitDe, Sonck, V., tkianai, yxNONG, Skalski, P., Hogan, A.,
949 Nair, D., strobel, M., Jain, M., 2022. ultralytics/yolov5: v7.0 - YOLOv5 SOTA Realtime
950 Instance Segmentation. <https://doi.org/10.5281/zenodo.7347926>
- 951 Kongkaew, C., Sakunrag, I., Chaiyakunapruk, N., Tawatsin, A., 2011. Effectiveness of citronella
952 preparations in preventing mosquito bites: systematic review of controlled laboratory
953 experimental studies. *Trop. Med. Int. Heal.* 16, 802–810. <https://doi.org/10.1111/j.1365-3156.2011.02781.x>
- 955 Kordali, S., Aslan, I., Çalmaşur, O., Cakir, A., 2006. Toxicity of essential oils isolated from three
956 *Artemisia* species and some of their major components to granary weevil, *Sitophilus*
957 *granarius* (L.) (Coleoptera: Curculionidae). *Ind Crop Prod* 23, 162–170.
958 <https://doi.org/10.1016/j.indcrop.2005.05.005>
- 959 Kulkarni, R.R., Pawar, P.V., Joseph, M.P., Akulwad, A.K., Sen, A., Joshi, S.P., 2013. *Lavandula*
960 *gibsoni* and *Plectranthus mollis* essential oils: chemical analysis and insect control activities
961 against *Aedes aegypti*, *Anopheles stephensi* and *Culex quinquefasciatus*. *J. Pest Sci.* 86, 713–
962 718. <https://doi.org/10.1007/s10340-013-0502-1>
- 963 Kwon, Y., Kim, S.H., Ronderos, D.S., Lee, Y., Akitake, B., Woodward, O.M., Guggino, W.B.,
964 Smith, D.P., Montell, C., 2010. *Drosophila* TRPA1 channel is required to avoid the naturally

965 occurring insect repellent citronellal. *Current biology* 20, 1672–1678.
966 <https://doi.org/10.1016/j.cub.2010.08.016>

967 Lahondère, C., Vinauger, C., Okubo, R.P., Wolff, G.H., Chan, J.K., Akbari, O.S., Riffell, J.A.,
968 2019. The olfactory basis of orchid pollination by mosquitoes. *Proceedings of the National*
969 *Academy of Sciences USA*. <https://doi.org/10.1073/pnas.1910589117>

970 Liang, Y., Li, J.L., Xu, S., Zhao, N.N., Zhou, L., Cheng, J., Liu, Z.L., 2013. Evaluation of
971 repellency of some chinese medicinal herbs essential oils against *Liposcelis bostrychophila*
972 (Psocoptera: Liposcelidae) and *Tribolium castaneum* (Coleoptera: Tenebrionidae). *J Econ*
973 *Entomol* 106, 513–519. <https://doi.org/10.1603/ec12247>

974 Liu, F., Wang, Q., Xu, P., Andreazza, F., Valbon, W.R., Bandason, E., Chen, M., Yan, R., Feng,
975 B., Smith, L.B., Scott, J.G., Takamatsu, G., Ihara, M., Matsuda, K., Klimavicz, J., Coats, J.,
976 Oliveira, E.E., Du, Y., Dong, K., 2021. A dual-target molecular mechanism of pyrethrum
977 repellency against mosquitoes. *Nat Commun* 12, 2553. [https://doi.org/10.1038/s41467-021-](https://doi.org/10.1038/s41467-021-22847-0)
978 [22847-0](https://doi.org/10.1038/s41467-021-22847-0)

979 Lu, T., Qiu, Y.T., Wang, G., Kwon, J.Y., Rutzler, M., Kwon, H.-W., Pitts, R.J., Loon, J.J.A.V.,
980 Takken, W., Carlson, J.R., Zwiebel, L.J., 2007. Odor coding in the maxillary palp of the
981 malaria vector mosquito *Anopheles gambiae*. *Current biology* 17, 1533–1544.
982 <https://doi.org/10.1016/j.cub.2007.07.062>

983 Lukhoba, C.W., Simmonds, M.S.J., Paton, A.J., 2006. *Plectranthus*: A review of ethnobotanical
984 uses. *J. Ethnopharmacol.* 103, 1–24. <https://doi.org/10.1016/j.jep.2005.09.011>

985 Maia, M.F., Moore, S.J., 2011. Plant-based insect repellents: a review of their efficacy,
986 development and testing. *Malaria journal* 10 Suppl 1, S11. [https://doi.org/10.1186/1475-2875-](https://doi.org/10.1186/1475-2875-10-s1-s11)
987 [10-s1-s11](https://doi.org/10.1186/1475-2875-10-s1-s11)

988 Majeed, S., Hill, S.R., Birgersson, G., Ignell, R., 2016. Detection and perception of generic host
989 volatiles by mosquitoes modulate host preference: context dependence of (R)-1-octen-3-ol.
990 *Royal Society open science* 3, 160467. <https://doi.org/10.1098/rsos.160467>

991 Majeed, S., Hill, S.R., Dekker, T., Ignell, R., 2017. Detection and perception of generic host
992 volatiles by mosquitoes: responses to CO2 constrains host-seeking behaviour. *Royal Society*
993 *open science* 4, 170189. <https://doi.org/10.1098/rsos.170189>

994 Matthews, B.J., Dudchenko, O., Kingan, S.B., Koren, S., Antoshechkin, I., Crawford, J.E.,
995 Glassford, W.J., Herre, M., Redmond, S.N., Rose, N.H., Weedall, G.D., Wu, Y., Batra, S.S.,
996 Brito-Sierra, C.A., Buckingham, S.D., Campbell, C.L., Chan, S., Cox, E., Evans, B.R.,
997 Fansiri, T., Filipović, I., Fontaine, A., Gloria-Soria, A., Hall, R., Joardar, V.S., Jones, A.K.,
998 Kay, R.G.G., Kodali, V.K., Lee, J., Lycett, G.J., Mitchell, S.N., Muehling, J., Murphy, M.R.,
999 Omer, A.D., Partridge, F.A., Peluso, P., Aiden, A.P., Ramasamy, V., Rašić, G., Roy, S.,
1000 Saavedra-Rodriguez, K., Sharan, S., Sharma, A., Smith, M.L., Turner, J., Weakley, A.M.,
1001 Zhao, Z., Akbari, O.S., Black, W.C., Cao, H., Darby, A.C., Hill, C.A., Johnston, J.S.,

1002 Murphy, T.D., Raikhel, A.S., Sattelle, D.B., Sharakhov, I.V., White, B.J., Zhao, L., Aiden,
1003 E.L., Mann, R.S., Lambrechts, L., Powell, J.R., Sharakhova, M.V., Tu, Z., Robertson, H.M.,
1004 McBride, C.S., Hastie, A.R., Korlach, J., Neafsey, D.E., Phillippy, A.M., Vosshall, L.B.,
1005 2018. Improved reference genome of *Aedes aegypti* informs arbovirus vector control. *Nature*
1006 563, 501–507. <https://doi.org/10.1038/s41586-018-0692-z>

1007 McMeniman, C.J., Corfas, R.A., Matthews, B.J., Ritchie, S.A., Vosshall, L.B., 2014. Multimodal
1008 integration of carbon dioxide and other sensory cues drives mosquito attraction to humans.
1009 *Cell* 156, 1060–1071. <https://doi.org/10.1016/j.cell.2013.12.044>

1010 Mei, Y., Li, L., Fan, L., Fan, W., Liu, L., Zhang, F., Hu, Z., Wang, K., Yang, L., Wang, Z., 2023.
1011 The history, stereochemistry, ethnopharmacology and quality assessment of borneol. *J*
1012 *Ethnopharmacol* 300, 115697. <https://doi.org/10.1016/j.jep.2022.115697>

1013 Melo, N., Capek, M., Arenas, O.M., Afify, A., Yilmaz, A., Potter, C.J., Laminette, P.J., Para, A.,
1014 Gallio, M., Stensmyr, M.C., 2021. The irritant receptor TRPA1 mediates the mosquito
1015 repellent effect of catnip. *Curr Biol*. <https://doi.org/10.1016/j.cub.2021.02.010>

1016 Melo, N., Wolff, G.H., Costa-da-Silva, A.L., Arribas, R., Triana, M.F., Gugger, M., Riffell, J.A.,
1017 Degennaro, M., Stensmyr, M.C., 2020. Geosmin attracts *Aedes aegypti* mosquitoes to
1018 oviposition sites. *Current Biology* 30, 1–8. <https://doi.org/10.1016/j.cub.2020.11.011>

1019 Moore, S.J., Debboun, M., 2007. History of Insect Repellents. Chapter 1. In *Insect Repellents:*
1020 *Principles, Methods, and Uses*. Eds: Debboun, M., Frances, S.P., Strickman, D. CRC Press.

1021 Ng, R., Wu, S., Su, C., 2020. Neuronal compartmentalization: a means to integrate sensory input
1022 at the earliest stage of information processing? *Bioessays* 42, e2000026.
1023 <https://doi.org/10.1002/bies.202000026>

1024 Nunes, R.K.V., Martins, U.N., Brito, T.B., Nepel, A., Costa, E.V., Barison, A., Santos, R.L.C.,
1025 Cavalcanti, S.C.H., 2018. Evaluation of (–)-borneol derivatives against the Zika vector, *Aedes*
1026 *aegypti* and a non-target species, *Artemia* sp. *Environ Sci Pollut R* 25, 31165–31174.
1027 <https://doi.org/10.1007/s11356-018-2809-1>

1028 Pålsson, K., Jaenson, T.G.T., 1999. Plant products used as mosquito repellents in Guinea Bissau,
1029 West Africa. *Acta Trop* 72, 39–52. [https://doi.org/10.1016/s0001-706x\(98\)00083-7](https://doi.org/10.1016/s0001-706x(98)00083-7)

1030 Picollo, M.I., Toloza, A.C., Cueto, G.M., Zygadlo, J., Zerba, E., 2008. Anticholinesterase and
1031 pediculicidal activities of monoterpenoids. *Fitoterapia* 79, 271–278.
1032 <https://doi.org/10.1016/j.fitote.2008.01.005>

1033 Pitarokili, D., Michaelakis, A., Koliopoulos, G., Giatropoulos, A., Tzakou, O., 2011. Chemical
1034 composition, larvicidal evaluation, and adult repellency of endemic Greek *Thymus* essential
1035 oils against the mosquito vector of West Nile virus. *Parasitol Res* 109, 425–430.
1036 <https://doi.org/10.1007/s00436-011-2271-1>

1037 Pratiwi, M.A.M., Purwati, 2021. The repellent activity test of rosemary leaf (*Rosmarinus*
1038 *officinalis*) essential oil gel preparations influence on *Aedes aegypti* mosquito. J Phys Conf
1039 Ser 1788, 012016. <https://doi.org/10.1088/1742-6596/1788/1/012016>

1040 Raj, G.A., Chandrasekaran, M., Krishnamoorthy, S., Jayaraman, M., Venkatesalu, V., 2015.
1041 Phytochemical profile and larvicidal properties of seed essential oil from *Nigella sativa* L.
1042 (Ranunculaceae), against *Aedes aegypti*, *Anopheles stephensi*, and *Culex quinquefasciatus*
1043 (Diptera: Culicidae). Parasitol Res 114, 3385–3391. [https://doi.org/10.1007/s00436-015-](https://doi.org/10.1007/s00436-015-4563-3)
1044 [4563-3](https://doi.org/10.1007/s00436-015-4563-3)

1045 Rajkumar, S., Jebanesan, A., 2010. Chemical composition and larvicidal activity of leaf essential
1046 oil from *Clausena dentata* (Willd) M. Roam. (Rutaceae) against the chikungunya vector,
1047 *Aedes aegypti* Linn. (Diptera: Culicidae). J Asia-pac Entomol 13, 107–109.
1048 <https://doi.org/10.1016/j.aspen.2010.02.001>

1049 Santos, S.R.L., Silva, V.B., Melo, M.A., Barbosa, J.D.F., Santos, R.L.C., Sousa, D.P. de,
1050 Cavalcanti, S.C.H., 2010. Toxic effects on and structure-toxicity relationships of
1051 phenylpropanoids, terpenes, and related compounds in *Aedes aegypti* larvae. Vector-Borne
1052 Zoonotic Dis. 10, 1049–1054. <https://doi.org/10.1089/vbz.2009.0158>

1053 Shankar, S., McMeniman, C.J., 2020. An updated antennal lobe atlas for the yellow fever
1054 mosquito *Aedes aegypti*. Plos Neglect Trop D 14, e0008729.
1055 <https://doi.org/10.1371/journal.pntd.0008729>

1056 Stensmyr, M.C., Dweck, H.K.M., Farhan, A., Ibba, I., Strutz, A., Mukunda, L., Linz, J., Grabe,
1057 V., Steck, K., Lavista-Llanos, S., Wicher, D., Sachse, S., Knaden, M., Becher, P.G., Seki, Y.,
1058 Hansson, B.S., 2012. A conserved dedicated olfactory circuit for detecting harmful microbes
1059 in *Drosophila*. Cell 151, 1345–1357. <https://doi.org/10.1016/j.cell.2012.09.046>

1060 Su, C.-Y., Menuz, K., Reisert, J., Carlson, J.R., 2012. Non-synaptic inhibition between grouped
1061 neurons in an olfactory circuit. Nature 492, 66–71. <https://doi.org/10.1038/nature11712>

1062 Takken, W., Kline, D.L., 1989. Carbon dioxide and 1-octen-3-ol as mosquito attractants. Journal
1063 of the American Mosquito Control Association 5, 311–316.

1064 Team, R.C., 2021. R: A language and environment for statistical computing. R Foundation for
1065 Statistical Computing, Vienna, Austria.

1066 Vinauger, C., Breugel, F. van, Locke, L.T., Tobin, K.K.S., Dickinson, M.H., Fairhall, A.L.,
1067 Akbari, O.S., Riffell, J.A., 2019. Visual-olfactory integration in the human disease vector
1068 mosquito *Aedes aegypti*. Current biology 29, 2509–2516.e5.
1069 <https://doi.org/10.1016/j.cub.2019.06.043>

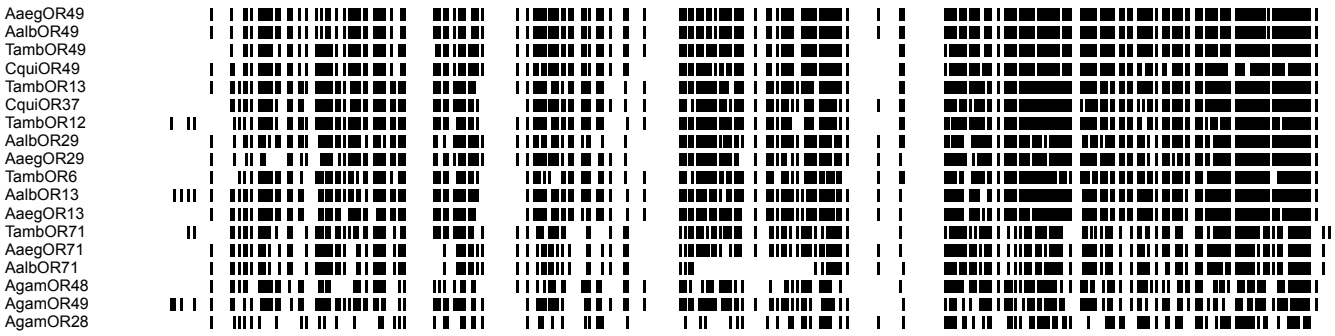
1070 Wadley, L., Sievers, C., Bamford, M., Goldberg, P., Berna, F., Miller, C., 2011. Middle stone
1071 age bedding construction and settlement patterns at Sibudu, South Africa. Science 334, 1388–
1072 1391. <https://doi.org/10.1126/science.1213317>

- 1073 Waliwitiya, R., Kennedy, C.J., Lowenberger, C.A., 2009. Larvicidal and oviposition □ altering
1074 activity of monoterpenoids, trans □ anithole and rosemary oil to the yellow fever mosquito
1075 *Aedes aegypti* (Diptera: Culicidae). Pest Manag Sci 65, 241–248.
1076 <https://doi.org/10.1002/ps.1675>
- 1077 Wang, G., Carey, A.F., Carlson, J.R., Zwiebel, L.J., 2010. Molecular basis of odor coding in the
1078 malaria vector mosquito *Anopheles gambiae*. PNAS 107.
1079 <https://doi.org/10.1073/pnas.0913392107>
- 1080 Wang, Y., Chen, Q., Guo, J., Li, J., Wang, J., Wen, M., Zhao, H., Ren, B., 2017. Molecular basis
1081 of peripheral olfactory sensing during oviposition in the behavior of the parasitic wasp
1082 *Anastatus japonicus*. Insect Biochem. Mol. Biol. 89, 58–70.
1083 <https://doi.org/10.1016/j.ibmb.2017.09.001>
- 1084 Wolff, G.H., Lahondère, C., Vinauger, C., Rylance, E., Riffell, J.A., 2023. Neuromodulation and
1085 differential learning across mosquito species. Proc. R. Soc. B 290, 20222118.
1086 <https://doi.org/10.1098/rspb.2022.2118>
- 1087 Xu, P., Zeng, F., Bedoukian, R.H., Leal, W.S., 2019. DEET and other repellents are inhibitors of
1088 mosquito odorant receptors for oviposition attractants. Insect Biochemistry and Molecular
1089 Biology 113, 103224. <https://doi.org/10.1016/j.ibmb.2019.103224>
- 1090 Zeng, F., Xu, P., Tan, K., Zarbin, P.H.G., Leal, W.S., 2018. Methyl dihydrojasmonate and lilial
1091 are the constituents with an “off-label” insect repellence in perfumes. Plos One 13, e0199386.
1092 <https://doi.org/10.1371/journal.pone.0199386>
- 1093 Zhang, N., Tang, L., Hu, W., Wang, K., Zhou, Y., Li, H., Huang, C., Chun, J., Zhang, Z., 2014.
1094 Insecticidal, fumigant, and repellent activities of sweet wormwood oil and its individual
1095 components against red imported fire ant workers (Hymenoptera: Formicidae). J Insect Sci
1096 14, 241. <https://doi.org/10.1093/jisesa/ieu103>
- 1097 Zhao, Z., Zung, J.L., Hinze, A., Kriete, A.L., Iqbal, A., Younger, M.A., Matthews, B.J., Merhof,
1098 D., Thiberge, S., Ignell, R., Strauch, M., McBride, C.S., 2022. Mosquito brains encode unique
1099 features of human odour to drive host seeking. Nature 1–7. <https://doi.org/10.1038/s41586-022-04675-4>
1100
- 1101 Zhou, X., Rinker, D.C., Pitts, R.J., Rokas, A., Zwiebel, L.J., 2014. Divergent and conserved
1102 elements comprise the chemoreceptive repertoire of the non-blood feeding mosquito
1103 *Toxorhynchites amboinensis*. Genome biology and evolution 6, 2883–2896.
1104 <https://doi.org/10.1093/gbe/evu231>
- 1105 Zhu, J.J., Cermak, S.C., Kenar, J.A., Brewer, G., Haynes, K.F., Boxler, D., Baker, P.D., Wang,
1106 D., Wang, C., Li, A.Y., Xue, R., Shen, Y., Wang, F., Agramonte, N.M., Bernier, U.R., Filho,
1107 J.G. de O., Borges, L.M.F., Friesen, K., Taylor, D.B., 2018. Better than DEET repellent
1108 compounds derived from coconut oil. Sci. Rep. 8, 14053. <https://doi.org/10.1038/s41598-018-32373-7>
1109

1110

A

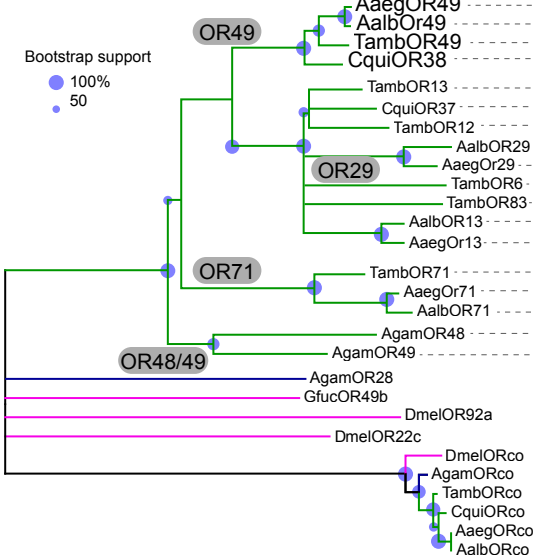
bioRxiv preprint doi: <https://doi.org/10.1101/2023.08.01.548307>; this version posted August 3, 2023. The copyright holder for this preprint (which was not certified by peer review) is the author/funder, who has granted bioRxiv a license to display the preprint in perpetuity. It is made available under aCC-BY-NC-ND 4.0 International license.



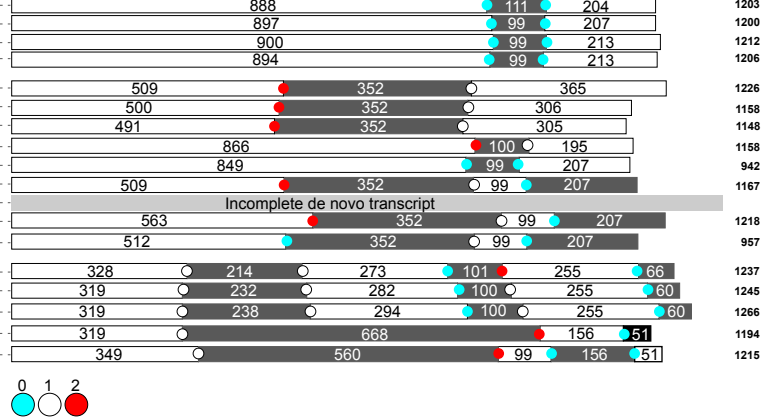
B

	Aalb Or49	Tamb Or49	Cqui 38	Tamb 13	Cqui 37	Tamb 12	Aalb 29	Aaeg 29	Tamb 6	Aalb 13	Aaeg 13	Tamb 71	Aaeg 71	Aalb 71	Agam 48	Agam 49	Agam 28
AaegOr49	98	89	81	65	65	62	58	58	60	61	60	53	50	43	50	52	39
AalbOr49		89	80	65	64	62	57	58	59	61	59	52	50	42	50	53	39
TambOR49			83	65	64	64	59	59	59	62	61	54	52	45	51	55	40
CquiOR38				64	63	64	59	59	59	62	61	55	52	45	51	56	41
TambOR13					79	79	75	74	73	77	76	54	51	44	53	55	39
CquiOR37						76	69	69	71	76	76	51	51	43	50	53	38
TambOR12							69	69	67	71	72	52	51	42	48	53	38
AalbOR29								83	66	68	68	52	52	45	48	50	38
AaegOR29									67	68	69	51	50	42	48	51	38
TambOR6										73	73	49	48	40	49	49	37
AalbOR13											91	52	52	44	50	52	39
AaegOR13												51	50	42	49	51	38
TambOR71													74	64	48	51	36
AaegOR71														78	48	48	36
AalbOR71															43	42	33
AgamOR48																57	36
AgamOR49																	37

C



D



E



F

